*Journal of Sound and Vibration* (2002) **251**(2), 193–214
doi:10.1006/jsvi.2001.4002, available online at http://www.idealibrary.com on IDEAL®

# STATISTICAL ENERGY ANALYSIS OF COUPLED PLATE SYSTEMS WITH LOW MODAL DENSITY AND LOW MODAL OVERLAP

C. HOPKINS

*Acoustics Centre, BRE, Garston, Watford WD25 9XX, England. E-mail: hopkinsc@bre.co.uk*

(*Received* 27 *April* 2001)

Finite element methods, experimental statistical energy analysis (ESEA) and Monte Carlo methods have been used to determine coupling loss factors for use in statistical energy analysis (SEA). The aim was to use the concept of an ESEA ensemble to facilitate the use of SEA with plate subsystems that have low modal density and low modal overlap. An advantage of the ESEA ensemble approach was that when the matrix inversion failed for a single deterministic analysis, the majority of ensemble members did not encounter problems. Failure of the matrix inversion for a single deterministic analysis may incorrectly lead to the conclusion that SEA is not appropriate. However, when the majority of the ESEA ensemble members have positive coupling loss factors, this provides sufficient motivation to attempt an SEA model. The ensembles were created using the normal distribution to introduce variation into the plate dimensions. For plate systems with low modal density and low modal overlap, it was found that the resulting probability distribution function for the linear coupling loss factor could be considered as lognormal. This allowed statistical confidence limits to be determined for the coupling loss factor. The SEA permutation method was then used to calculate the expected range of the response using these confidence limits in the SEA matrix solution. For plate systems with low modal density and low modal overlap, relatively small variation/uncertainty in the physical properties caused large differences in the coupling parameters. For this reason, a single deterministic analysis is of minimal use. Therefore, the ability to determine both the ensemble average and the expected range with SEA is crucial in allowing a robust assessment of vibration transmission between plate systems with low modal density and low modal overlap.



## 1. INTRODUCTION

Prediction of structure-borne sound transmission is of importance in many fields of noise control including building, ship, automobile and aerospace engineering. Although each field has its own particular sound transmission problems, engineers generally use two main techniques for the analysis of vibration transmission in built-up structures, statistical energy analysis (SEA) [1] and finite element methods (FEM) [2]. These approaches are described as statistical and deterministic methods respectively.

A problem common to many areas of structural dynamics but of particular relevance to building acoustics is the prediction of structure-borne sound transmission between plates with low modal density and low modal overlap. In building acoustics, there is a clearly defined frequency range of interest, 50 Hz–5 kHz, from which third octave band data are used to calculate single-number quantities [3] for regulatory purposes. In this range,

0022-460X/02/120193 + 22 $35.00/0 

concrete/masonry walls or floors have mode counts in third octave bands ranging from zero up to a few hundred.

For some structures, it is possible to carry out all relevant analysis using either a deterministic or a statistical approach. More commonly, information is required across a frequency range that encompasses both low- and high-frequency ranges. When both approaches are required, the question arises as to which model to use in the mid-frequency range. One possibility is to maintain a clear distinction between the two approaches and improve the process of transferring the geometry, dimensions and material properties of the structure between the different models as well as facilitating the merge of the output data. Another possibility has been proposed by Langley and Bremner [4] that uses fuzzy structure theory and incorporates features of both statistical and deterministic approaches. However, for the low- and mid-frequency ranges, uncertainty in the material properties and dimensions means that a single deterministic analysis (using local or global modes) will rarely predict the large fluctuations in the same frequency bands as in the measured response. It is for this reason that response statistics are desirable for the low- and mid-frequency ranges. The approach investigated in this paper is to use the SEA framework with coupling parameters and statistical confidence limits determined from FEM data. The aim is to allow statistical information from a number of deterministic analyses to be used in the SEA framework, and hence calculate the expected range of response for coupled plates with low modal density and low modal overlap.

In classical SEA, wave theory is often used to estimate the coupling losses between structural systems consisting of simple beams and plates. Assuming that the junctions have been correctly modelled, it is useful to know the requirements on the subsystems such that these estimates will apply to the ensemble with a low variance. Computational [5, 6] and physical [7] experiments on beams and plates have indicated that the coupling loss factor (CLF) will approximate that predicted from wave theory transmission coefficients when the larger of the modal overlap factors ($M$) for two coupled elements is greater than or equal to unity. For plates, Fahy and Mohammed [5] apply an extra condition that there should be a mode count ($N$) of at least five modes in the frequency band. In general, the condition $N \geqslant 5$ forms a useful quantitative definition of the term "multi-modal". Mace and Rosenberg [8] have since shown that for coupled rectangular plates, the coupling strength depends on a coupling parameter, $\gamma_0$, rather than the modal overlap factor. However, although it is not exact, the modal overlap factor remains a practical indicator of coupling strength because of its ease of calculation. Hence, the conditions $M \geqslant 1$ and $N \geqslant 5$ can be used to *estimate* as to when SEA wave theory is "appropriate" for plate systems. When these conditions are not met, SEA can still be used but it must be accepted that errors of unknown magnitude can occur. It is for this reason that deterministic analysis such as FEM has been investigated in the literature [e.g., references 8–13] to determine SEA coupling parameters between coupled plates. The underlying aim has generally been to elucidate and potentially avoid the limitations of classical SEA. The majority of previous work on FEM used a single deterministic analysis to calculate coupling parameters rather than providing the basis for a statistical approach as used in this paper.

## 2. ANALYSIS USING FEM, ESEA, THE ESEA ENSEMBLE AND SEA

This section describes the approach taken to determine vibration transmission between plates with low modal density and low modal overlap. This approach uses FEM, ESEA and Monte Carlo methods to calculate CLFs for use in predictive SEA. These CLFs and their associated statistics are then used to determine minimum and maximum subsystem energy ratios in a process that will be referred to as the "SEA permutation method".

### 2.1. SEA PERMUTATION METHOD

SEA assumes a statistical description of the subsystems such that the subsystem response represents the ensemble average of "similar" subsystems with physical parameters drawn from statistical distributions. This ensemble is referred to as the SEA ensemble. Plate subsystems can be described in SEA using mass, stiffness, internal damping, thickness, area and the coupling line lengths. Information on the exact plate geometry and dimensions can be renounced because of the uncertainty in describing the modal features of multi-modal subsystems at high frequencies.

With ESEA, there is the potential to create a different kind of ensemble, which will be termed an ESEA ensemble. Like the SEA ensemble, the ESEA ensemble considers systems that consist of subsystems with "similar" properties. However, unlike the SEA ensemble, it can include subsystems where the SEA assumption of equipartition of modal energy in a frequency band (i.e., incident energy uniformly distributed in angle) does not apply, but ESEA "weak" coupling still exists (from Smith's [14] definition of "weak" coupling which ensures a well-conditioned matrix for ESEA matrix inversions).

The SEA ensemble considers uncertainty in the description of the modal features. In contrast, the ESEA ensemble is intended for subsystems where there is limited knowledge about the modal features, but uncertainty as to how the eigenfrequencies will be distributed amongst the frequency bands of interest. The ESEA ensemble can therefore be used for "similar" sets of structures that have high tolerances on the dimensions and material properties. For these structures, a single deterministic analysis is likely to be of limited use.

The following example is used to illustrate a potential application of the ESEA ensemble to buildings. Similar examples could be found for ship, automobile and aerospace engineering. This example concerns the prediction of vibration transmission in third octave bands between adjacent dwellings for a set of "similar" dwellings. The required output of the study is the vibration of the walls and floors in terms of the mean response as well as the expected range of the response. It is the latter output that is expected to be of particular interest. The subsystem modal density is low because the walls and floors are composed of thick masonry/concrete plates. Also, mode-wave duality indicates that the range of equivalent angles for the low-frequency modes is restricted by the rectangular subsystem geometry [15]. For these reasons, equipartition of modal energy in a frequency band does not occur in these plate subsystems. However, for the set of "similar" dwellings there will be variations due to workmanship, material properties and plate dimensions such that any certainty regarding the equivalent angles is counteracted by the uncertainty in the prediction of the eigenfrequencies and eigenfunctions at low frequencies. The requirement for third octave bands exacerbates the low-frequency problem because "similar" plates in a set of "similar" dwellings can have zero, one, or more than one eigenfrequency in the same third octave band.

One approach to this study would be to use predictive SEA with CLF values determined from angular average wave theory. However, large errors can occur due to incorrect CLF values because of low modal density and low modal overlap [5]. Also, the output would only be the mean response. This is due to the lack of formal procedures in SEA to determine the expected range of the response for these subsystems. Typical variations in material properties and plate dimensions in the set of "similar" dwellings are likely to have negligible effect on the plate energy or the wave theory CLF values in the SEA model because of the relatively large plate sizes. For this reason and the strong modal dependence that can be expected in the CLF, the repeated use of SEA wave theory models with variations to the material properties and plate dimensions of the subsystems will *not* create a realistic range for the response.

The approach considered in this paper is to use FEM and ESEA to determine CLF values for isolated L- and T-junctions of rectangular plates that can be used in larger SEA models comprising these junctions. It is intended to use this approach at frequencies above the fundamental global eigenfrequency of the isolated junction.

The ESEA ensemble represents coupled plate junctions in the set of "similar" dwellings by taking account of the variation in material properties and dimensions. To use this approach, SEA must be appropriate for the system under study. This can be indicated during the ESEA analysis by the ability to determine positive coupling and internal loss factors, and by well-conditioned energy matrices. The advantage of ESEA with numerical experiments is that both the mean and variance of the ensemble average CLF are found without including the effect of sampling errors in the plate energy that can be significant with physical experiments. Therefore, the mean response for the ESEA ensemble can be obtained and there is an opportunity to calculate the expected range of the response. The latter can be found by ascribing statistical confidence limits to the CLF values such that each CLF can take two values corresponding to the lower and upper limits. These can be used in a series of SEA models including all possible permutations of the confidence limits for all the CLF values. The number of permutations for the SEA model is equal to $2^n$, where $n$ is the number of CLF values that have lower and upper confidence limits. Although the number of permutations soon increases with many coupled subsystems, matrix solutions are sufficiently fast such that this approach will be feasible for small numbers of subsystems. It may also be useful with SEA models where the majority of CLF values are single values determined from wave theory and only a small number of CLF values have confidence limits. The final step is to find the expected range of the response from the minimum and maximum subsystem energy ratios. This approach to determine minimum and maximum subsystem energy ratios will be referred to as the "SEA permutation method". For engineering purposes, the energy ratios are converted and displayed using $D_{v,ij}$, the vibration level difference in decibels between source subsystem $i$ and receiver subsystem $j$.

## 2.2. FEM ANALYSIS

FEM analyses were carried out using ANSYS 5.5 software with the SHELL63 element. Element dimensions were $< \lambda_B/6$ where the bending wavelength, $\lambda_B$, corresponded to the plate with the smallest $\lambda_B$ value.

Rain-on-the-roof excitation was applied over all the unconstrained nodes on one surface of the source plate with forces of unity magnitude and random phase. With numerical realization of rain-on-the-roof, it is possible to have different sets of random phase values for the unity magnitude input forces, i.e., different "rainfall". Therefore, different sets of random phase values were used for each member of the ensemble such that the ensemble output can be considered as representative of different physical realizations of rain-on-the-roof.

In the FEM model, the loss factor is introduced in terms of the constant damping ratio, and is purely an internal loss in the FEM calculations. However, to simulate the total loss factor (TLF) that occurs with fully connected walls in complete buildings, the loss factor needs to represent the sum of the coupling loss factors (for a plate that is fully connected in a building) plus the internal loss factor [10]. It should be noted that this scenario is quite different from that of thin metal or perspex plates that are commonly dealt with in the literature [e.g., references 9, 12, 13], where the TLF is dominated by internal damping. The loss factor used in the FEM model for all test constructions was $1/\sqrt{f}$ and was based upon the typical value for the sum of the coupling loss factors for concrete/masonry walls in

a typical dwelling as described by Craik [16]. To avoid a significant decrease in vibration with distance across each subsystem, the loss factor did not include a frequency-independent internal loss factor [15].

### 2.3. EXPERIMENTAL SEA

The aim of ESEA is to use the SEA power-balance equations to determine the loss factors through inversion of the energy matrix. Lyon [17] proposed the technique and highlighted the main problems. Problems can occur because of errors in the measured energies that can give negative CLF values due to ill-conditioned matrices. Woodhouse [18] emphasized two important points regarding ESEA. Firstly, ESEA verifies that SEA is suitable to analyze a system before using SEA to assess the effect of any changes. Secondly, the development of ESEA is crucial in allowing experimental determination of coupling losses across complex junctions for which theoretical solutions are often inaccurate or simply do not exist.

The system under analysis is considered as a set of ESEA subsystems. The general ESEA matrix is determined from the general SEA matrix and is shown in equation (1) where $E_{ij}$ is the energy of subsystem $i$ with power input into subsystem $j$, $\eta_{ij}$ is the CLF from subsystem $i$ to subsystem $j$, $\eta_{ii}$ is the internal loss factor (ILF) of subsystem $i$, and $\Pi_{in,i}$ is the power input to subsystem $i$.

$$\begin{bmatrix} \sum_{n=1}^{N} \eta_{1n} & -\eta_{21} & -\eta_{31} & \cdots & -\eta_{N1} \\ -\eta_{12} & \sum_{n=1}^{N} \eta_{2n} & -\eta_{32} & & \vdots \\ -\eta_{13} & -\eta_{23} & \sum_{n=1}^{N} \eta_{3n} & & \\ \vdots & & & \ddots & \\ -\eta_{1N} & & & & \sum_{n=1}^{N} \eta_{Nn} \end{bmatrix} \begin{bmatrix} E_{11} & E_{12} & E_{13} & \cdots & E_{1N} \\ E_{21} & E_{22} & E_{23} & & \\ E_{31} & E_{32} & E_{33} & & \vdots \\ \vdots & & & \ddots & \\ E_{N1} & & & & E_{NN} \end{bmatrix}$$

$$= \begin{bmatrix} \Pi_{in,1}/\omega & 0 & 0 & \cdots & \cdot \\ 0 & \Pi_{in,2}/\omega & 0 & & \\ 0 & 0 & \Pi_{in,3}/\omega & & \vdots \\ \vdots & & & \ddots & \\ 0 & & & & \Pi_{in,N}/\omega \end{bmatrix}. \tag{1}$$

Experimental determination of the subsystem energies and power inputs allows inversion of the energy matrix to determine the loss factor matrix. The subsystem energies are determined from numerical experiments using FEM. These experiments require the energies to be measured in all subsystems for sequential power injection into each subsystem. If a system has been partitioned into suitable subsystems, errors in the energy are negligible and there is ESEA "weak" coupling, the energy matrix should be well-conditioned. This is due to subsystem energy terms on the diagonal that are significantly larger than the off-diagonal terms. However, any numerical experiment can have errors in the measured energy values and therefore the matrix is prone to being ill-conditioned and to output negative ILF and/or CLF values.

Work on ESEA initially concentrated on the collection of accurate measurement data from physical experiments on systems that fulfilled the requirements of SEA. Bies and Hamid [19] successfully used ESEA to determine TLF and CLF values on a physical system composed of two coupled plates. Excitation was applied sequentially at a number of different points to resolve the issue [20] that single excitation points do not give rise to statistically independent modes. Physical experiments are generally carried out using single excitation points, which, for multi-modal subsystems with high damping (e.g., thin metal plates with damping layers) is not a significant problem as only a few single excitation points may be required to simulate statistically independent excitation forces. However, for subsystems that are not multi-modal (i.e., concrete/masonry plates), this highlights an advantage of numerical or analytical experiments in which rain-on-the roof excitation can be used to satisfy the requirement for statistically independent excitation forces.

Later work concentrated on improving matrix solutions to avoid the problems of negative CLF values. Woodhouse [18] demonstrated the sensitivity of matrix inversion to small errors and proposed the use of an iterative procedure to determine a symmetric matrix that satisfied the form of the SEA CLF matrix. Clarkson and Ranky [7] successfully used the same approach. It is important to note that the failure of the matrix inversion to produce positive CLF values does not prove that the system cannot or should not be modelled using SEA. Assuming that it is only the errors in the experimentally determined energies that cause the negative CLF values, the system may actually exhibit SEA behaviour. Therefore, the role of iterative matrix-fitting procedures can be seen as one of "forcing" SEA upon a system that may or may not have SEA behaviour. Hodges *et al.* [21] concentrated on the optimization of matrix-fitting routines in order to increase the chances of determining a loss factor matrix that could form the basis of an SEA model for the system.

Lalor [22] noted potential problems with any optimization approach in that the ability to significantly alter a CLF also implied that these optimized values might not be reliable. An alternative matrix solution was proposed by Lalor to overcome the problem of ill-conditioned ESEA matrices. Lalor's proposal was to split the calculation of CLF and ILF values into separate matrices as shown in equation (2). For the calculation of the CLF values with $N \geqslant 3$, this uses the smaller $(N-1)\times(N-1)$ energy matrix rather than the $N \times N$ energy matrix of the general ESEA matrix formulation.

$$\begin{bmatrix} \eta_{1i} \\ \vdots \\ \eta_{ri} \\ \vdots \\ \eta_{Ni} \end{bmatrix}_{r \neq i} = \frac{\Pi_{in,i}}{\omega E_{ii}} \begin{bmatrix} \left(\frac{E_{11}}{E_{i1}} - \frac{E_{1i}}{E_{ii}}\right) & \cdots & \left(\frac{E_{r1}}{E_{i1}} - \frac{E_{ri}}{E_{ii}}\right) & \cdots & \left(\frac{E_{N1}}{E_{i1}} - \frac{E_{Ni}}{E_{ii}}\right) \\ \vdots & \ddots & & & \vdots \\ \vdots & & \left(\frac{E_{rr}}{E_{ir}} - \frac{E_{ri}}{E_{ii}}\right) & & \vdots \\ \vdots & & & \ddots & \vdots \\ \left(\frac{E_{1N}}{E_{iN}} - \frac{E_{1i}}{E_{ii}}\right) & \cdots & \left(\frac{E_{rN}}{E_{iN}} - \frac{E_{ri}}{E_{ii}}\right) & \cdots & \left(\frac{E_{NN}}{E_{iN}} - \frac{E_{Ni}}{E_{ii}}\right) \end{bmatrix}^{-1} \begin{bmatrix} 1 \\ \vdots \\ \vdots \\ \vdots \\ 1 \end{bmatrix}$$

$$\begin{bmatrix} \eta_{11} \\ \vdots \\ \eta_{NN} \end{bmatrix} = \frac{1}{\omega} \begin{bmatrix} E_{11} & \cdots & E_{N1} \\ \vdots & \ddots & \vdots \\ E_{1N} & \cdots & E_{NN} \end{bmatrix}^{-1} \begin{bmatrix} \Pi_{in,1} \\ \vdots \\ \Pi_{in,N} \end{bmatrix}. \tag{2}$$

Another possibility is to use the fundamental SEA equations for two- or three-coupled subsystems to create specific ESEA matrices for the L- and T-junctions analyzed in this paper. The specific matrices for two-and three-coupled subsystems are shown in equations (3) and (4) respectively. These specific ESEA matrices are likely to be ill-conditioned and re-arranging the rows will not improve the matrix condition number. However, they are included for comparison with the general ESEA matrix and the alternative matrix formulation.

$$\begin{bmatrix} -E_{11} & -E_{11} & 0 & E_{21} \\ 0 & E_{11} & -E_{21} & -E_{21} \\ -E_{12} & -E_{12} & 0 & E_{22} \\ 0 & E_{12} & -E_{22} & -E_{22} \end{bmatrix} \begin{bmatrix} \eta_{1d} \\ \eta_{12} \\ \eta_{2d} \\ \eta_{21} \end{bmatrix} = \begin{bmatrix} -\Pi_{in,1}/\omega \\ 0 \\ 0 \\ -\Pi_{in,2}/\omega \end{bmatrix}. \tag{3}$$

$$\begin{bmatrix} -E_{11} & -E_{11} & -E_{11} & 0 & E_{21} & 0 & 0 & E_{31} & 0 \\ 0 & E_{11} & 0 & -E_{21} & -E_{21} & -E_{21} & 0 & 0 & E_{31} \\ 0 & 0 & E_{11} & 0 & 0 & E_{21} & -E_{31} & -E_{31} & -E_{31} \\ -E_{12} & -E_{12} & -E_{12} & 0 & E_{22} & 0 & 0 & E_{32} & 0 \\ 0 & E_{12} & 0 & -E_{22} & -E_{22} & -E_{22} & 0 & 0 & E_{32} \\ 0 & 0 & E_{12} & 0 & 0 & E_{22} & -E_{32} & -E_{32} & -E_{32} \\ -E_{13} & -E_{13} & -E_{13} & 0 & E_{23} & 0 & 0 & E_{33} & 0 \\ 0 & E_{13} & 0 & -E_{23} & -E_{23} & -E_{23} & 0 & 0 & E_{33} \\ 0 & 0 & E_{13} & 0 & 0 & E_{23} & -E_{33} & -E_{33} & -E_{33} \end{bmatrix} \begin{bmatrix} \eta_{1d} \\ \eta_{12} \\ \eta_{13} \\ \eta_{2d} \\ \eta_{21} \\ \eta_{23} \\ \eta_{3d} \\ \eta_{31} \\ \eta_{32} \end{bmatrix}$$

$$= \begin{bmatrix} -\Pi_{in,1}/\omega \\ 0 \\ 0 \\ 0 \\ -\Pi_{in,2}/\omega \\ 0 \\ 0 \\ 0 \\ -\Pi_{in,3}/\omega \end{bmatrix}. \tag{4}$$

It was anticipated that for plates with low modal density and low modal overlap, problems with the ESEA matrix inversion could be a barrier to the use of FEM ESEA and hence the SEA permutation method. For this reason, all three matrix formulations were investigated.

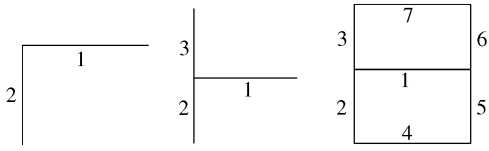


Figure 1. Plan view of FEM test constructions with subsystem numbers. L-junction (left), T-junction (middle), Seven-plate system (right).

TABLE 1

*FEM test construction data*

| | L-junction | | T-junction | | |
|---|---|---|---|---|---|
| Subsystem number | 1 | 2 | 1 | 2 | 3 |
| Density (kg/m$^3$) | 1400 | 600 | 2000 | 600 | 600 |
| $c_L$ (m/s$^1$) | 2200 | 1900 | 3200 | 1900 | 1900 |
| The Poisson ratio | 0·2 | 0·2 | 0·2 | 0·2 | 0·2 |
| Thickness (m) | 0·1 | 0·1 | 0·215 | 0·1 | 0·1 |
| $x$ (m) | 4·0 | 3·5 | 4·0 | 3·5 | 3·0 |
| $y$ (m)† | 2·4 | 2·4 | 2·4 | 2·4 | 2·4 |

†$y$-dimension corresponds to the junction line.

## 3. NUMERICAL EXPERIMENTS

### 3.1. FEM TEST CONSTRUCTIONS

Three constructions were used in the numerical experiments: L-junction, T-junction, and a seven-plate system formed from two T-junctions and four L-junctions. The subsystem numbering for the constructions is shown in Figure 1. The seven-plate system can be seen as representing masonry walls that form two adjacent rooms. It was formed from two T-junctions (walls 1, 2, 3, 5 and 6), two L-junctions (walls 2, 4 and 5) and two different L-junctions (walls 3, 6 and 7) where wall 7 is identical to wall 1.

The test construction data for the L- and T-junctions are shown in Table 1.

All constructions had simply supported plate boundaries and a simply supported junction line such that only bending waves were considered in the FEM model.

For each system the ESEA ensemble contained 30 members. The ensemble was created through the use of random numbers drawn from a normal distribution, $N(\mu, \sigma)$, to vary the plate length that was perpendicular to the junction for all plates. $N(\mu, \sigma)$ used the $x$-dimension in Table 1 as the mean value, $\mu$, with a standard deviation, $\sigma = 0{\cdot}25$ m. This gave a realistic $x$-dimension range for a set of "similar" dwellings.

For the L- and T-junctions, analysis was carried out for third octave bands, 50 Hz–1 kHz. However, to reduce computation time with the seven-plate system, analysis was only carried out for third octave bands in the range 50–200 Hz. The number of single frequencies used to determine third octave band data depended upon the modal overlap factor. To ensure that bands with low modal overlap were adequately represented, a large number of frequencies were used for $M < 1$. For the L-junction with $M < 1$, 1 Hz steps were used in each band. For the T-junction with $M < 0{\cdot}5$, 2 Hz steps were used in each band, For $M \geqslant 1$ ($L$-junction) and $M \geqslant 0{\cdot}5$ (T-junction), three frequencies were used in each band where one

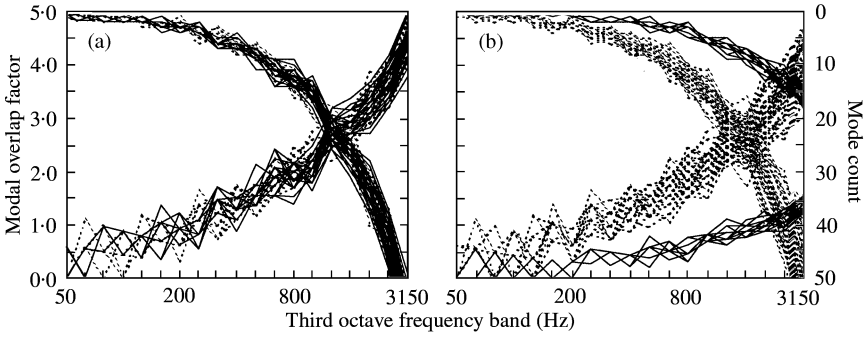


Figure 2. L-junction (left) and T-junction (right). Modal overlap factor (lower curves) and mode count( upper curves) for the ensemble of plate 1 (——, (a) and (b)) and plate 2 (....., (a)) and plates 2 and 3 (....., (b)).

frequency was the band centre frequency, with the other two frequencies equally spaced over the third octave bandwidth.

The modal overlap factor and local mode count (bending modes only) for the L- and T-junctions are shown in Figure 2. All ensemble members are shown, although it is not always possible to identify 30 curves because of identical values with some ensemble members. These figures show typical mode count and modal overlap data for concrete/masonry walls over the majority of the building acoustics frequency range, 50 Hz–3·15 kHz. However, to reduce computation time the FEM analysis for the L- and T-junctions only considered 50 Hz–1 kHz.

In order to make statements about the ensemble for each individual plate, it is convenient to refer to $M$ as the arithmetic mean of the ensemble's modal overlap factors and $N$ as the arithmetic mean of the ensemble's local mode counts. Hence, for the L-junction, the conditions $M \geqslant 1$ and $N \geqslant 5$ are satisfied in third octave bands $\geqslant 315$ Hz for plate 1 and $\geqslant 400$ Hz for plate 2. For the T-junction, the conditions $M \geqslant 1$ and $N \geqslant 5$ are satisfied in third octave bands $\geqslant 2{\cdot}5$ kHz for plate 1, and $\geqslant 400$ Hz for plates 2 and 3. It is worth noting that typical solid separating walls (i.e., T-junction, plate 1) have $M < 1$ and $N < 5$ over the majority of the building acoustics frequency range that predominantly determines the single-number quantity [3] used to rate airborne sound insulation. This indicates the potential restriction on the successful application of SEA wave theory to concrete/masonry structures. However, typical flanking walls (i.e., T-junction, plates 2 and 3 and L-junction, plate 2) and separating cavity wall leaves (i.e., L-junction, plate 1) can have $M < 1$ and $N < 5$ over a smaller frequency range.

### 3.2. ESEA MATRIX CONDITION

This section contains an assessment of ESEA errors and matrix condition numbers through comparison of the three ESEA matrix formulations:

(A) general ESEA matrix formulation,
(B) alternative ESEA matrix formulation (after Lalor [22]),
(C) specific two or three subsystem ESEA matrix formulations.

Formulations A and C were used for the L-junction and formulations A, B and C were used for the T-junction. (For $N$ subsystems, formulation B has an $(N-1)\times(N-1)$ energy matrix and can only be used for three or more subsystems.)

The first step is to note how many negative ILF values occurred in the ESEA process, because these have no physical meaning. In fact, *no* negative ILF values occurred for any members of the L- and T-junctions ensembles. To date [15], models of two L-junctions and two T-junctions have led to only *one* negative ILF, which was for *one* member of an ensemble, for *one* plate at *one* frequency, using *one* matrix formulation, A. This suggests that negative ILF values are unlikely to be common with these types of plate systems, which is beneficial to the ESEA ensemble approach because rejection of any ensemble members due to this problem is likely to be a rare occurrence. Therefore, any future consideration of matrix-fitting procedures [21] may only be required for a few members of the ensemble.

The ESEA energy matrices are square matrices and are denoted as **E**. A unique solution for the inverse of **E**, $\mathbf{E}^{-1}$ exists when **E** is non-singular. However, because of experimental errors in the energies and non-SEA behaviour of the system, $\mathbf{E}^{-1}$ can differ significantly with only small changes to the energy values. As an indicator of this problem, the condition number [23] of matrix **E**, $\kappa(\mathbf{E})$, can be used to measure the sensitivity of $\mathbf{E}^{-1}$ to small changes in the matrix entries of **E**. For ideal square matrices, the condition number is unity and the matrix problem is termed "well-conditioned". When the condition number is much larger than unity, the matrix problem is termed "ill-conditioned". Golub and Van Loan [23] demonstrate that the size of the determinant cannot be used as a measure of ill-conditioning because it is possible to have a well-conditioned matrix with a small determinant. It should be emphasized that different norms can be used to determine the condition number, and therefore the terms describing the matrix condition are dependent upon the norm used in the calculation. In this paper, only the Euclidean norm is used (also called the $L_2$-norm) to allow a comparison of the condition number for the three different matrix formulations.

The next step is to make the link between the condition number and the potential errors from the matrix inversion. Although it is possible to make this link with knowledge of the errors in the energy and input power matrices, upper error bounds [23] can give high overestimates that may not be particularly useful. In dealing with computational electromagnetics, Hafner [24] has noted that the condition number is not a robust guide to finding accurate solutions. At present, it seems to be appropriate simply to label to rank order the matrices as "well-conditioned" or "ill-conditioned" rather than trying to make links from the condition number to the errors in the loss factor matrix that may not be robust.

The minimum and maximum condition numbers in the ensemble are shown in Figure 3 for the L-junction with matrix formulations A and C, and the T-junction with matrix formulations A, B and C.

For the T-junction with matrix formulation B, condition numbers are determined for three energy matrices, each matrix being used to determine the CLF values *to* a subsystem. B(1) is used to determine $\eta_{21}$ and $\eta_{31}$, B(2) to determine $\eta_{12}, \eta_{32}$, and B(3) to determine $\eta_{13}$ and $\eta_{23}$. Figure 3 shows the minimum and maximum values of B(1) and B(2 and 3). The latter set is formed by combining B(2) and B(3) and is justifiable because plates 2 and 3 are similar.

For the L-junction, matrix formulation A gave lower condition numbers than C. Also, there were *no* negative CLF values produced by any of the matrix formulations and the condition numbers remained relatively low when $M < 1$ and $N < 5$. This provides evidence to support the hypothesis of Woodhouse [18] that SEA should always be applicable to two subsystems when only one subsystem is excited. Therefore, it may be possible to extend this hypothesis to plate systems that have low modal density and low modal overlap.

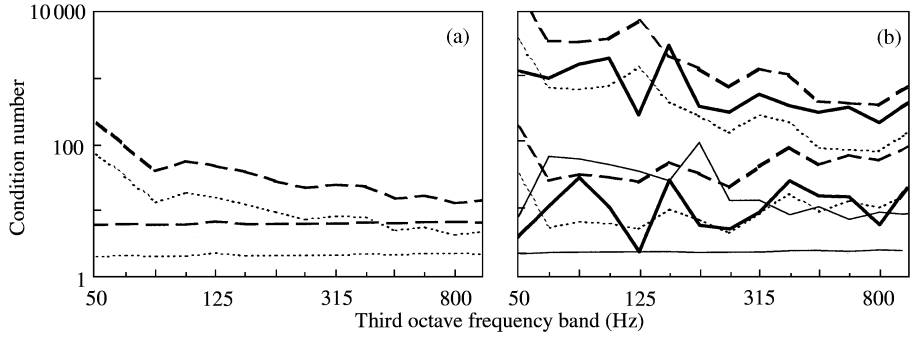


Figure 3. L-junction (left) and T-junction (right). Minimum and maximum condition numbers of the ESEA ensemble for matrix formulations A (....., (a) and (b)); B(1) (——, (b)); B (2 and 3) (————, (b)); C(– – –, (a) and (b)).

For the T-junction, the condition numbers are, in general, significantly higher than for the L-junction. Formulation B(1) had condition numbers similar to those for the L-junction, whereas all other condition numbers were generally higher. It is seen that formulation B(1) can be advantageous in obtaining lower condition numbers than formulation A or C. However, the condition numbers indicate that when formulation B is used to determine CLF values that are significantly different in magnitude, the condition numbers can be relatively high and similar to A and C. This occurred for B(2) where $\eta_{12} \gg \eta_{32}$, and B(3) when $\eta_{13} \gg \eta_{23}$.

For transmission around the corner of the T-junctions, *no* negative CLF values were produced by any of the matrix formulations. However, there were negative CLF values for transmission across the straight section of the T-junctions with up to eight of the 30 ensemble members, in 11 of the 14 third octave bands between 50 Hz and 1 kHz. It was noted that regardless of the matrix formulation, the negative CLF values occurred for the same ensemble members at the same frequencies.

Although no simple link exists between the condition number and the potential errors from the matrix inversion, the ESEA matrix formulation with the lowest condition numbers can be considered as the most robust formulation for which an SEA model is appropriate. General matrix formulation A, typically gives the lowest condition numbers and is therefore considered as the most robust formulation. In contrast, specific matrix formulation C gives the highest condition numbers and for this reason is not recommended for ESEA. For most purposes, general formulation A gives adequately low condition numbers. However, alternative formulation B can be used to give even lower condition numbers when the CLF values are both high. For this reason, alternative matrix formulation B is recommended when problems are encountered with general formulation A *before* attempting matrix-fitting routines [21].

The trend with these systems was that the condition number tended to increase with the number of subsystems. This suits the original intention to use FEM and ESEA with systems comprising only a small number of subsystems, e.g., L- or T-junctions.

To date [15], negative CLF values have only occurred for transmission across the straight section of T-junctions. For the T-junction in this paper, up to eight of the 30 ensemble members gave negative CLF values in *some* third octave bands. Therefore, there is a relatively high success rate in determining positive CLF values. This highlights a significant benefit of the ESEA ensemble approach over that of a single deterministic analysis from which the latter might lead to the conclusion that SEA is not appropriate. When the majority of the ESEA ensemble members have positive CLF values, this provides

sufficient motivation to attempt an SEA model. However, matrix-fitting procedures [21] could of course be used to avoid *any* negative CLF values in the ensemble.

### 3.3. STATISTICAL DISTRIBUTIONS OF THE COUPLING LOSS FACTOR

The aim in this section is to investigate the probability distribution of the CLF ensemble that was determined from FEM and ESEA.

In numerical experiments on coupled rectangular plates by Fahy and Mohammed [5], an ensemble was created using subsystem dimension ratios randomly chosen from a normal distribution. It was noted that when the modal overlap was less than unity, the use of normally distributed input parameters for the ensemble gave rise to distinctly non-normal distributions of the ensemble outputs. Fahy and Mohammed concluded that it is "… impossible to estimate confidence limits from a knowledge, or estimate of the standard deviation alone, at low values of $M$. This fact alone is sufficient to limit severely the practical utility of SEA under conditions of low modal overlap". The outputs analyzed in their numerical studies were coupling loss factors and power flow normalized on the input power, which had right or left skewed distributions. For low modal overlap ($M < 1$), the distributions for coupling loss factors between coupled beams and between coupled plates were both right skewed. The existence of right skewed distributions with systems of low modal overlap is perhaps of less concern than suggested by these authors, because it is standard practise in acoustics to deal with response data in decibels. It will be shown in this paper that for coupled plates with low modal density and low modal overlap, it *is* possible to estimate confidence limits and that it is sometimes appropriate to determine the ESEA ensemble average using a logarithmic average.

Manohar and Keane [25] carried out numerical experiments on coupled one-dimensional subsystems and concluded that either lognormal or gamma distributions adequately described the probability density function for the dissipated power. However, they noted that further work was needed to justify the choice of these distributions. Wester and Mace [26, 27] carried out numerical experiments to investigate ensemble averages for two coupled rectangular plates. This gave rise to some probability density functions for the logarithm of the normalized power flow that were right skewed [27]. Considering these data along with those of Hodges and Woodhouse [28], and Fahy and Mohammed [5] it is likely that any resulting probability density function could be system specific, as well as specific to the choice of coupling parameter, method of ensemble creation, excitation, subsystem type and the choice of local or global mode analysis.

In this paper, the probability distribution of the CLF data is required before the mean, standard deviation and confidence intervals can be used in further SEA calculations. The ensemble was created using a normal distribution to describe the variation in plate length and therefore the findings are only applicable to this ensemble. From the observations of Fahy and Mohammed [5] for plate systems with low modal overlap, there is no reason to assume that the resulting CLF data will also have a normal distribution. The first step is to assess the normality of the linear CLF using normal quantile plots. If these distributions are found to be right-skewed, then a logarithmic transformation can be applied to determine if the linear CLF ensemble can be described as a lognormal distribution.

The normal quantile plots with both linear and logarithmic CLF values are shown in Figures 4 and 5 for the L- and T-junctions respectively. From Fahy and Mohammed, it is expected that non-normal distributions will occur when $M < 1$. However, no rigid rule has yet been established as to whether this applies to the modal overlap factor for the source plate, receiver plate or the geometric mean for the coupled plates. The latter may not be

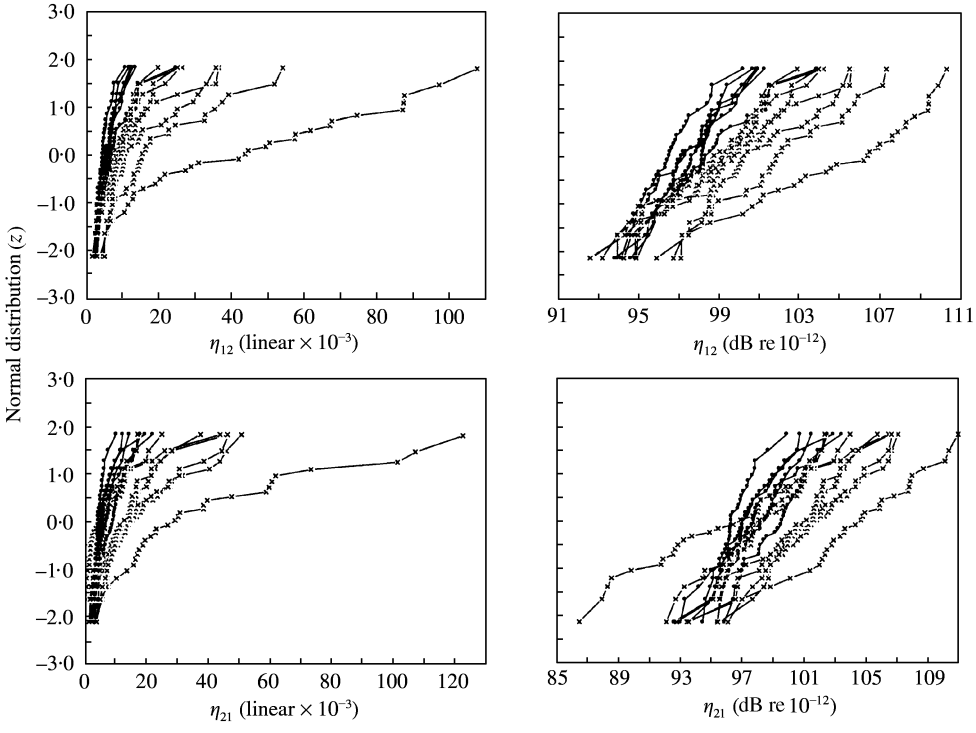


Figure 4. L-junction. Normal quantile plots for linear and dB data, 50 Hz–1 kHz (14 curves). —×— indicates $M < 1$ for plates 1 and 2.

sufficient in all cases [15]. One possible criterion would be that $M < 1$ for all plates coupled along the same junction line, where $M$ is the arithmetic mean of the ensemble's modal overlap factors. However, in the figures in this section, a slightly less strict requirement is used for which the criterion is $M < 1$ for subsystems $i$ and $j$ that are involved in $\eta_{ij}$. This is indicated using —×— for each frequency band where $M < 1$. This only differs from the other criterion in that $\eta_{23}$ would otherwise have —×— for all third octave bands.

For both junctions, the figures illustrate that when $M < 1$, the distributions of the linear CLF are widest and there can be significant right skew such that it is appropriate to attempt a logarithmic transformation. The transformation gives rise to sufficiently straight lines such that for engineering purposes the linear CLF can be described as a lognormal distribution. When $M \geqslant 1$, the linear CLF data can generally be considered as a normal distribution, although there is still some evidence of right skew that could be due to the fluctuations in the relatively small ensemble. Therefore, to calculate statistical parameters from these data, the logarithmic transformation is used regardless of the value of the modal overlap factor.

For the logarithmic CLF of the T-junction, a few of the lowest CLF values do not appear to belong to the normal distribution (e.g., the two $\eta_{21}$ values of 71·9 and 74·0 dB, and also the $\eta_{23}$ value of 44·6 dB). The only feature that these values share in common is that they have significantly higher or lower condition numbers than those at adjacent frequencies. If the condition numbers had been consistently higher, then this would have provided a reason to treat these values as outliers. However, this assumes that the condition number can be considered as a robust measure.

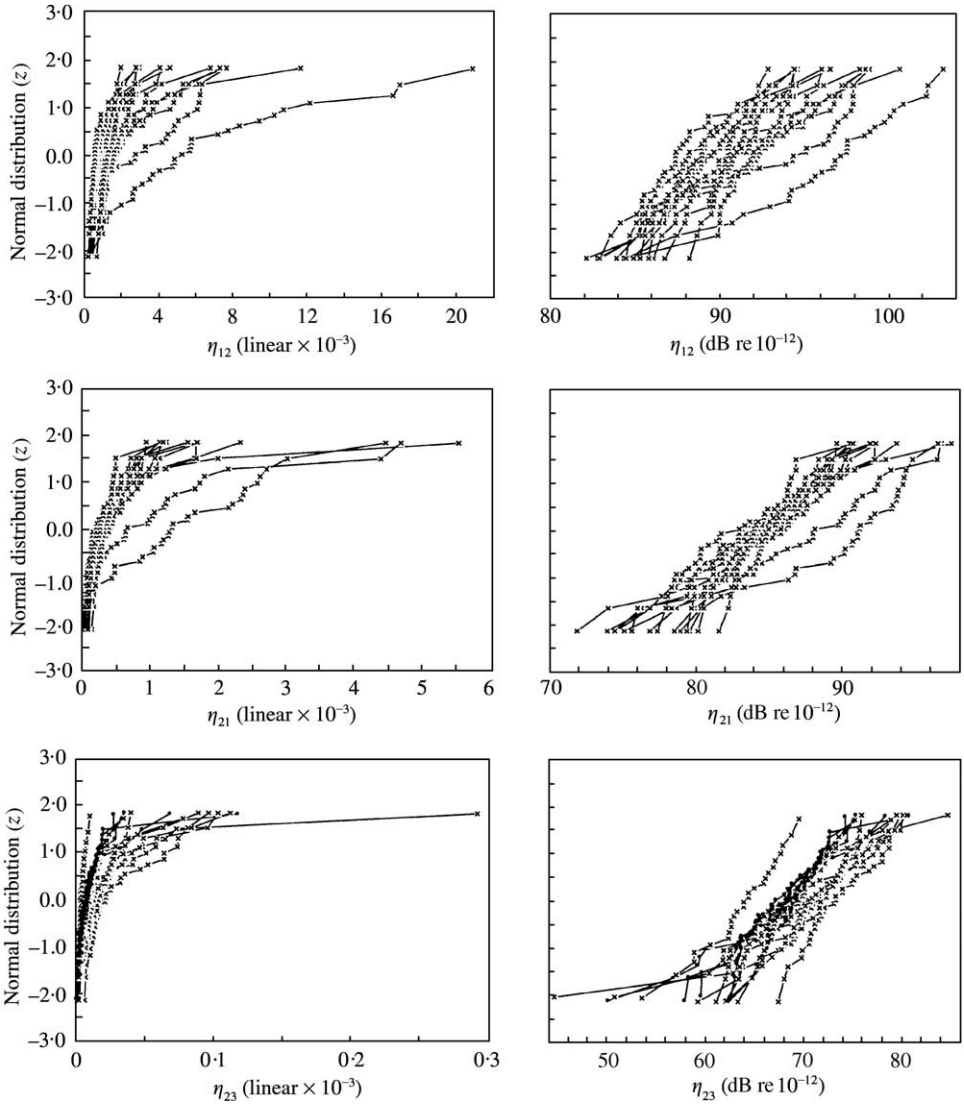


Figure 5. T-junction. Normal quantile plots for linear and dB data, 50 Hz–1 kHz (14 curves). —×— indicates $M < 1$ for plates 1 and 2 with $\eta_{12}$ and $\eta_{21}$, and plates 2 and 3 with $\eta_{23}$.

As a general conclusion, when $M < 1$ for all plates that share the same junction line, the linear CLF is likely to have a lognormal distribution and when $M \gg 1$, it can generally be assumed to have a normal distribution. In all cases, but particularly where the modal overlap falls between these two ranges, the normal quantile plots can be used to assess the statistical distribution.

The implications of a lognormal distribution for the linear CLF are now considered with reference to its intended use in predictive SEA using either the full matrix solution or path analysis. The latter can be used to aid investigations into the relative importance of the different transmission paths. For any system with power injected into subsystem 1, the energy ratio between subsystem 1 and subsystem $N$ for transmission along the path

1, 2, 3, 4, …, $N$ is shown as

$$E_1/E_N = (\eta_2\eta_3\eta_4, \ldots, \eta_N)/(\eta_{12}\eta_{23}\eta_{34}, \ldots, \eta_{(N-1)N}). \quad (5)$$

Path analysis poses no problem to the use of the mean, standard deviation and confidence limits of the CLF in logarithmic form. However, this is not the case with the matrix solution for which linear values are required. Therefore, a reverse transformation is needed to convert the mean and standard deviation back to linear values along with a method to calculate confidence limits in linear units.

The normal distribution $N(\mu, \sigma)$ has two parameters, $\mu$ and $\sigma$ and is referred to as a two-parameter distribution. The lognormal distribution [29] is generally a three-parameter distribution $\Lambda(\tau, \mu, \sigma)$, where $\tau$ is the lowest possible value (referred to as the threshold) that can exist in the lognormal distribution. Assuming that the linear CLF can potentially be zero [11] or infinitesimally small, then $\tau = 0$ and its lognormal distribution can be described by a two-parameter distribution $\Lambda(\mu, \sigma)$.

To discuss the reverse transformation of the mean and standard deviation, the lognormal distribution of the linear CLF is now denoted as $\Lambda(\mu_\Lambda, \sigma_\Lambda)$ and the normal distribution of the logarithmic CLF as $N(\mu, \sigma)$. For engineering purposes, it is common to describe the CLF in decibels using a formula such as $10\lg(\eta_{ij}/10^{-12})$. However, to determine the mean and standard deviation in linear values, it is more convenient here to use $\lg(\eta_{ij})$ for the normal distribution, $N(\mu, \sigma)$. Having determined $\mu$ and $\sigma$, the reverse transformation is $\mu_\Lambda = 10^\mu$ and $\sigma_\Lambda = 10^\sigma$. From the transformation process, $\mu_\Lambda$ is the geometric mean of the linear values and $\sigma_\Lambda$ can be described as the geometric standard deviation. When the sample mean is approximately equal to the population mean and the sample standard deviation is approximately equal to the population standard deviation, the lower and upper confidence limits of the linear CLF are $\mu_\Lambda/(\sigma_\Lambda)^n$ and $\mu_\Lambda(\sigma_\Lambda)^n$, respectively, where $n = 1$ for the 68% interval, $n = 2$ for the 95% interval and $n = 3$ for the 99·7% interval. For small samples, Student-$t$ procedures can be used to determine $n$.

The evidence in this section (albeit limited) confirms that there is potential in the use of the ESEA ensemble for plate subsystems with low modal density and low modal overlap. The ability to determine statistical parameters that describe the normal distribution of the logarithmic CLF facilitates its use with quick path analysis calculations using decibels. More importantly, the ability to determine statistical parameters (mean, standard deviation and confidence intervals) that describe the lognormal distribution of the linear CLF facilitates its inclusion in predictive SEA using the matrix solution. In the next section, the expected range of $D_{v,ij}$ is determined by using the CLF 95% confidence limits in the SEA permutation method.

### 3.4. SEA PERMUTATION METHOD: L- AND T-JUNCTIONS

In this section, the L- and T-junctions are used to assess the SEA permutation method. For the T-junction, transmission between plate 1 and plate 2 (or 3) is referred to as "transmission around the corner", whereas transmission between plates 2 and 3 is referred to as "transmission across the straight section".

The ensemble of FEM $D_{v,ij}$ data is compared with minimum and maximum $D_{v,ij}$ data that have been determined from the SEA permutation method using the 95% confidence limits of the FEM ESEA CLF. Although this may appear to be a circular verification route for the FEM ESEA approach, it allows an initial check on the matrix inversion and the assumption of a lognormal distribution for the linear CLF as well as confirming that the

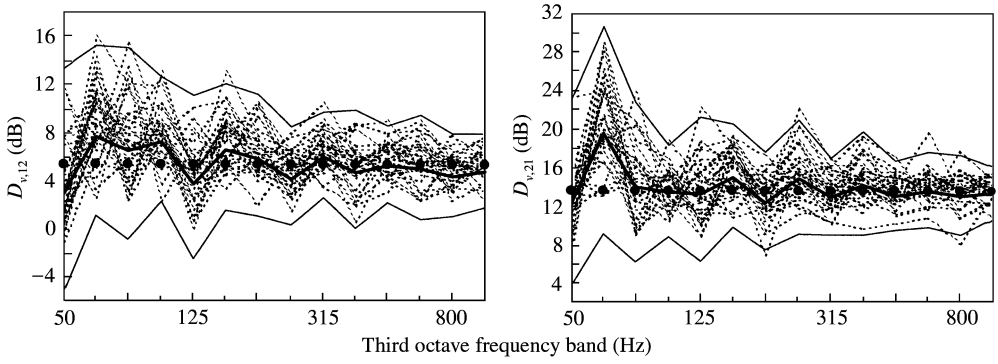


Figure 6. L-junction. Vibration level difference, $D_{v,ij}$ (source plate: $i$, receiver plate: $j$). FEM ensemble (30 dotted lines). SEA predictions using wave theory (black circles). FEM ESEA CLF ensemble average (thick solid line). Expected range from the SEA permutation method (two thin solid lines).

SEA permutation method is appropriate. It also allows an opportunity to assess the differences between the ensemble average, the ensemble members and the prediction from SEA bending wave theory.

The $D_{v,ij}$ data are shown for the L-junction in Figure 6 and for the T-junction in Figure 7. From the large range of the FEM ensemble data, it is apparent that a single deterministic analysis would be of minimal use, even though the level of uncertainty in the description of the plates is not atypical.

The figures indicate that when $M < 1$ and $N < 5$, $D_{v,ij}$ from SEA wave theory is still a reasonable approximation for the FEM ensemble average $D_{v,ij}$. However, it is important to note that this does not occur in general [5, 8, 30] and is due in part to the relatively high damping. Of particular note is the observation that the range of the FEM ensemble can be similar in magnitude to $D_{v,ij}$ from SEA wave theory. This highlights the need to be able to determine the expected range of $D_{v,ij}$. In general, the minimum and maximum $D_{v,ij}$ data from the SEA permutation method are seen to provide a satisfactory estimate of the expected range.

For transmission around the corner of the L- and T-junctions, the minimum $D_{v,ij}$ value tends to be a slight underestimate when $M < 1$ and $N < 5$ and can be considered to err on the side of caution. However, for transmission across the straight section of the T-junction, the underestimate for 50–160 Hz is more significant, with the largest underestimate at 125 Hz ($M < 1$ and $N < 5$). The latter problem is due to the $\eta_{23}$ outlier of 44·6 dB identified in the normal quantile plot (Figure 5). However, for 50–160 Hz, the lognormal distribution was a reasonable approximation.

It is concluded that, in combination, there are no major problems with matrix inversion errors, the assumption of a lognormal distribution, and the SEA permutation method. However, it appears that underestimation of the minimum $D_{v,ij}$ value can sometimes be significant when $M < 1$ and $N < 5$.

The final stage can now be carried out in the next section by testing the SEA permutation method with a larger plate system consisting of these isolated L- and T-junctions.

### 3.5. SEA PERMUTATION METHOD: SEVEN-PLATE SYSTEM

A more demanding test of the SEA permutation method is now made through analysis of the seven-plate system. This plate system was used to test the SEA permutation method

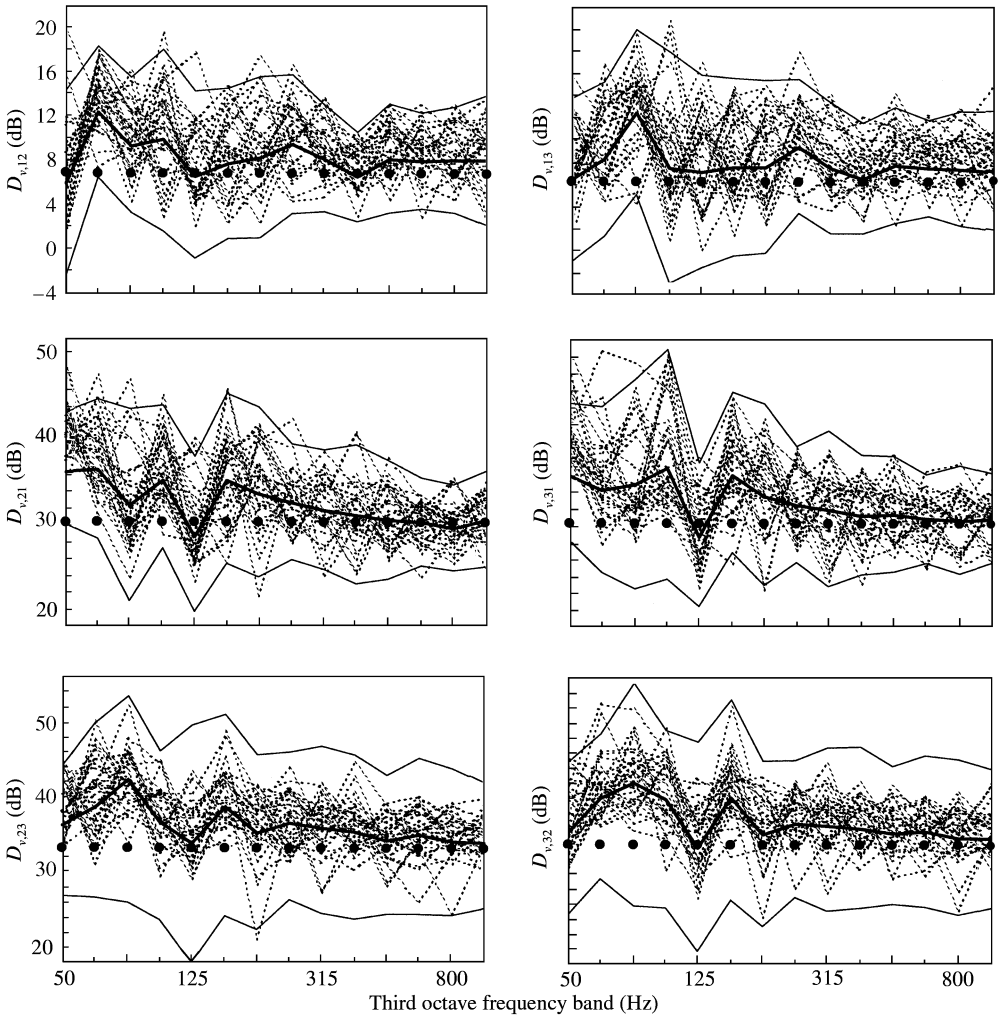


Figure 7. T-junction. Vibration level difference, $D_{v,ij}$ (source plate: $i$, receiver plate: $j$). FEM ensemble (30 dotted lines). SEA predictions using wave theory (black circles). FEM ESEA CLF ensemble average (thick solid line). Expected range from the SEA permutation method (two thin solid lines).

using the CLF 95% confidence intervals. (The FEM model used the loss factor $1/\sqrt{f}$ for each plate, as was used for each of the isolated L- and T-junctions that formed this seven-plate system.)

The $D_{v,ij}$ data are shown in Figure 8. The three main findings are: (1) the expected range tends to account for the range of the individual ensemble members, (2) $D_{v,ij}$ from SEA bending wave theory is a reasonable approximation for the FEM ensemble average $D_{v,ij}$ for this system, and (3) the ensemble average $D_{v,ij}$ calculated using the FEM ESEA CLF in an SEA model generally describes the FEM ensemble average $D_{v,ij}$.

When the receiver subsystem is directly coupled to the source subsystem, the minimum and maximum $D_{v,ij}$ data can provide a satisfactory estimate of the expected range (see $D_{v,13}$, $D_{v,24}$, $D_{v,31}$ and $D_{v,37}$). However, there is still a general underestimation of the minimum $D_{v,ij}$ value with significant underestimation in some cases (see $D_{v,12}$, $D_{v,21}$, $D_{v,23}$ and $D_{v,32}$).

When the receiver subsystem is *not* directly coupled to the source subsystem, the SEA permutation method can give rise to significant underestimates for the minimum $D_{v,ij}$ values (see $D_{v,26}$), and significant overestimates for the maximum $D_{v,ij}$ values (see $D_{v,14}$ and $D_{v,17}$).

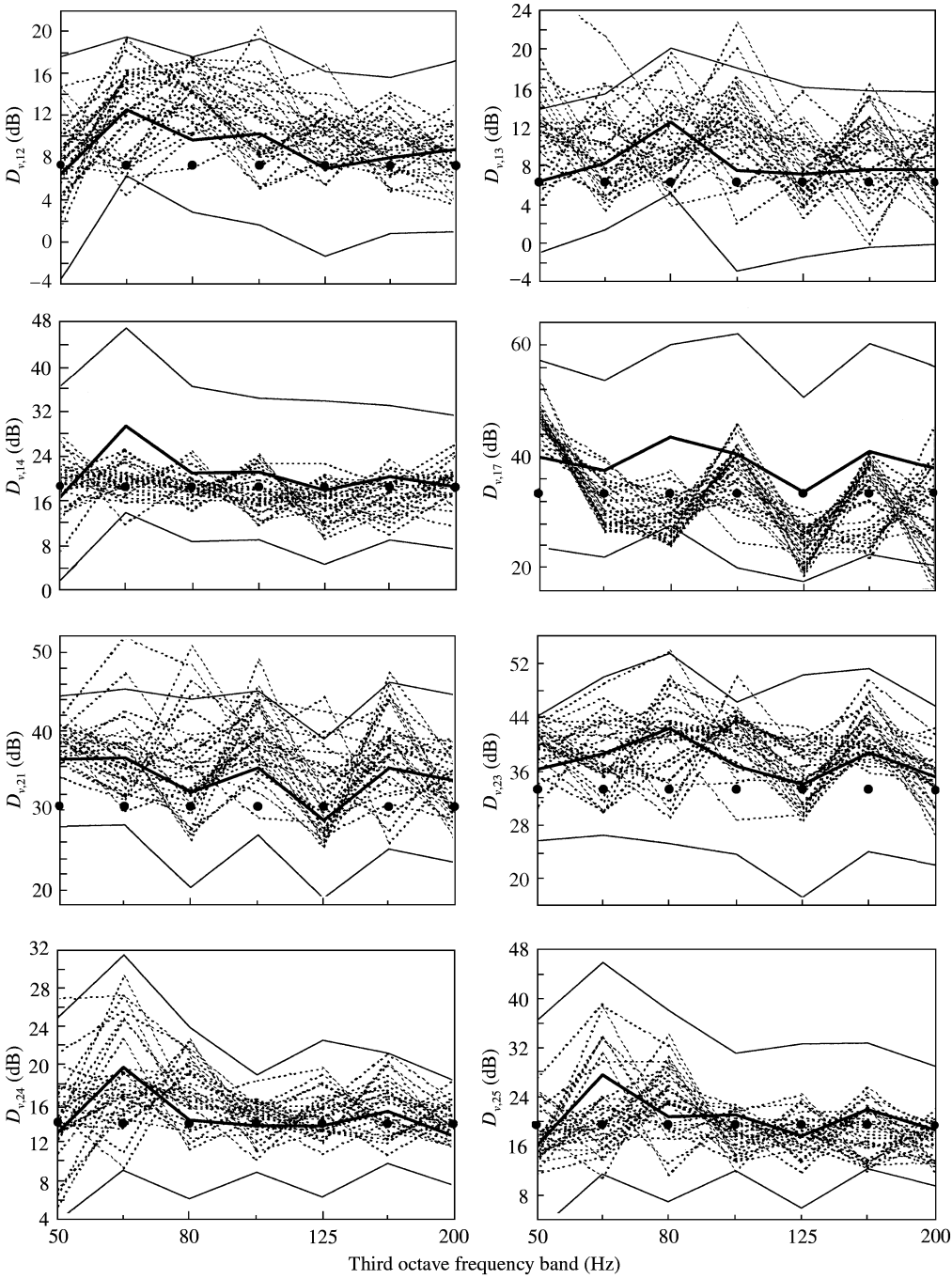


Figure 8. Seven-plate system. Vibration level difference, $D_{v,ij}$ (source plate: $i$, receiver plate: $j$). FEM ensemble (30 dotted lines). SEA predictions using wave theory (black circles). FEM ESEA CLF ensemble average (thick solid line). Expected range from the SEA permutation method (two thin solid lines).

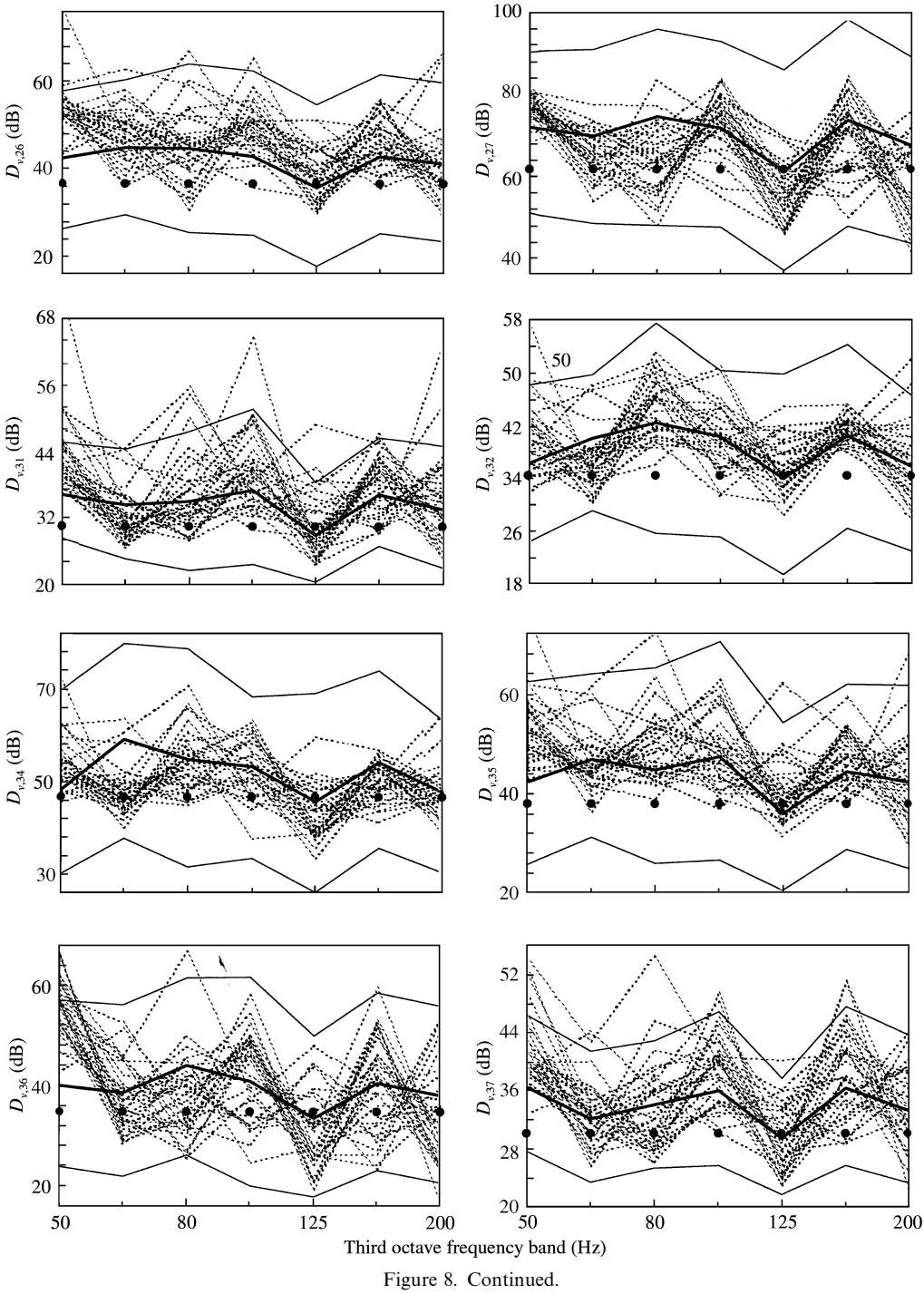


Figure 8. Continued.

Recalling that smaller underestimates of the minimum $D_{v,ij}$ values occurred with the isolated L- and T-junctions, these underestimates are likely to be caused by an accumulation of errors because the vibration transmission now takes place across more than one junction.

Some problems concerning the use of CLF data determined from isolated L- and T-junctions in complete systems are to be expected because the complete system will have different global eigenfrequencies to the isolated junctions. The global eigenfrequencies are important because the peaks in the coupling tend to occur at global eigenfrequencies [15, 30]. However, use of the ESEA ensemble to randomly shift the global eigenfrequencies of the isolated component systems has been shown here to provide a useful estimate of the vibration transmission and the ensemble statistics. In general, the SEA permutation method tends to err on the side of caution. In a favourable light, this could be seen as beneficial because a robust solution should certainly not underestimate the expected range. However, significant errors can occur when the receiver subsystem is *not* directly coupled to the source subsystem.

## 4. CONCLUSIONS

The results demonstrate that use of the ESEA ensemble enables plate systems with low modal density and low modal overlap to be included in the framework of SEA. It has also been shown that to determine CLF data for use in predictive SEA, it is advantageous to use the ESEA ensemble, rather than a single deterministic analysis. This is because relatively small variations (e.g., $<10\%$) in the physical properties of plate systems with low modal density and low modal overlap can cause large differences in the coupling parameters. For this reason, a single deterministic analysis is considered to be of minimal use in many practical situations where there is uncertainty is the material properties and dimensions. Another significant advantage of the ESEA ensemble is that when the matrix inversion fails for a single deterministic analysis, it has been found that problems are unlikely to be encountered with the majority of ESEA ensemble members. In contrast, when the matrix inversion fails for a single deterministic analysis, this may incorrectly lead to the conclusion that SEA is not appropriate at all. When the majority of the ESEA ensemble members have positive CLF values, this provides sufficient motivation to attempt an SEA model. However, matrix-fitting procedures [21] could still be used to avoid *any* negative CLF values in the ensemble.

Problems with the ESEA matrix inversion were anticipated to be a potential barrier to the successful application of FEM ESEA. However, it was found that there were no significant problems with negative ILF or CLF values for these plate systems despite the relatively high condition numbers when the modal density and modal overlap was low. (For more general applications of ESEA to plates with low modal density and low modal overlap, it should be noted that the lack of problems from the matrix inversion in this paper could be due to the relatively high damping used for the masonry/concrete plates.) It was concluded that to obtain the lowest condition numbers, the general ESEA matrix formulation should be used, although in some cases, lower condition numbers can be achieved using Lalor's alternative matrix formulation. The specific ESEA matrix formulations gave the highest condition numbers and should therefore be avoided.

Concerning the statistics of the FEM ESEA CLF, it was shown that for these particular ensembles, the probability distribution function for the linear CLF could be considered as lognormal. (This finding is only expected to apply when a normal distribution is used to create the ensemble.) This enabled calculation of the statistics of the linear CLF and use of the SEA permutation method to determine the expected range of $D_{v,ij}$. The test constructions were isolated L- and T-junctions and a plate system formed from these isolated junctions. The SEA permutation method using the CLF 95% confidence intervals was most suited to situations where the receiver subsystem was directly coupled to the source subsystem and an estimate was required that erred on the side of caution for the

expected range. When the receiver subsystem is *not* directly coupled to the source subsystem, the expected range *can* be significantly overestimated.

It is concluded that there is potential in the SEA permutation method to determine the expected range of response with plate systems that have low modal density and low modal overlap. However, more numerical experiments are required to investigate the limitations of this approach.

## ACKNOWLEDGMENT

The author would like to thank Professor R. J. M. Craik (Heriot-Watt University) for his advice in the preparation of the thesis that formed the basis for this paper.

## REFERENCES

1. R. H. Lyon and R. G. DeJong 1995 *Theory and Application of Statistical Energy Analysis*. London: Butterworth Heinemann; Second edition.
2. O. C. Zienkiewicz 1997 *The Finite Element Method*. London: McGraw-Hill Company.
3. Anon. BS EN ISO 717–1:1997 Acoustics—rating of sound insulation in buildings and of building elements. Part 1. Airborne sound insulation.
4. R. S. Langley and P. Bremner 1999 *Journal of the Acoustical Society of America* **105**, 1657–1671 A hybrid method for the vibration analysis of complex structural–acoustic systems.
5. F. J. Fahy and A. D. Mohammed 1992 *Journal of Sound and Vibration* **158**, 45–67. A study of uncertainty in applications of SEA to coupled beam and plate systems. Part 1: computational experiments.
6. H. G. Davies and M. A. Wahab 1981 *Journal of Sound and Vibration* **77**, 311–321. Ensemble averages of power flow in randomly excited coupled beams.
7. B. L. Clarkson and M. F. Ranky 1984 *Journal of Sound and Vibration* **94**, 249–261. On the measurement of the coupling loss factor of structural connections.
8. B. R. Mace and J. Rosenberg 1998 *Journal of Sound and Vibration* **212**, 395–415. The SEA of two coupled plates: an investigation into the effects of subsystem irregularity.
9. C. Simmons 1991 *Journal of Sound and Vibration* **144**, 215–227. Structure-borne sound transmission through plate junctions and estimates of SEA coupling loss factors using the finite element method.
10. J. A. Steel and R. J. M. Craik 1994 *Journal of Sound and Vibration* **178**, 553–561. Statistical energy analysis of structure-borne sound transmission by finite element methods.
11. F. F. Yap and J. Woodhouse 1996 *Journal of Sound and Vibration* **197**, 351–371. Investigation of damping effects on statistical energy analysis of coupled structures.
12. C. R. Fredo 1997 *Journal of Sound and Vibration* **199**, 645–666. A SEA-like approach for the derivation of energy flow coefficients with a finite element model.
13. B. R. Mace and P. J. Shorter 2000 *Journal of Sound and Vibration* **233**, 369–389. Energy flow models from finite element analysis.
14. P. W. Smith 1979 *Journal of the Acoustical Society of America* **65**, 695–698. Statistical models of coupled dynamical systems and transition from weak to strong coupling.
15. C. Hopkins 2000 *Ph.D. Thesis*, *Heriot-Watt University*. Structure-borne sound transmission between coupled plates.
16. R. J. M. Craik 1981 *Applied Acoustics* **14**, 347–359. Damping of building structures.
17. R. H. Lyon 1975 *Statistical Energy Analysis of Dynamic Systems*: *Theory and Applications*. Cambridge: MIT Press.
18. J. Woodhouse 1981 *Applied Acoustics* **14**, 455–469. An introduction to statistical energy analysis of structural vibration.
19. D. A. Bies and S. Hamid 1980 *Journal of Sound and Vibration* **70**, 187–204. In situ determination of loss and coupling loss factors by the power injection method.
20. F. J. Fahy 1970 *Journal of Sound and Vibration* **11**, 481–483. Energy flow between oscillators: special case of point excitation.
21. C. H. Hodges, P. Nash and J. Woodhouse 1987 *Applied Acoustics* **22**, 47–69. Measurement of coupling loss factors by matrix fitting: an investigation of numerical procedures.

22. N. LALOR 1990 *ISVR Technical Report No*. 182, *June* 1990. Practical considerations for the measurement of internal and coupling loss factors on complex structures.
23. G. H. GOLUB and C. F. VAN LOAN 1989 *Matrix Computations*. Baltimore, MD: The John Hopkins University Press; second edition.
24. C. HAFNER 1999 *Post-modern Electromagnetic*: *Using Intelligent Maxwell Solvers*. New York: John Wiley & Sons Ltd.
25. C. S. MANOHAR and A. J. KEANE 1994 *Philosphical Transactions of the Royal Society of London*, *Series A* **346**, 525–542. Statistics of energy flows in spring-coupled one-dimensional subsystems.
26. E. C. N. WESTER and B. R. MACE 1996 *Journal of Sound and Vibration* **193**, 793–822. Statistical energy analysis of two edge-coupled rectangular plates: ensemble averages.
27. E. C. N. WESTER and B. R. MACE 1999 *Proceedings of Inter-Noise*'99, *Fort Lauderdale*, *Florida*, *U.S.A*. Ensemble statistics of energy flow in very irregular systems using a wave approach.
28. C. H. HODGES and J. WOODHOUSE 1989 *Journal of Sound and Vibration* **130**, 237–268. Confinement of vibration by one-dimensional disorder, I: theory of ensemble averaging, II: a numerical experiment on different ensemble averages.
29. E. L. CROW and K. SHIMIZU (editors) 1988 *Lognormal Distributions*: *Theory and Applications*. New York: Marcel Dekker Inc.
30. R. J. M. CRAIK, J. A. STEEL and D. I. EVANS 1991 *Journal of Sound and Vibration* **144**, 95–107. Statistical energy analysis of structure-borne sound transmission at low frequencies.